

Determination of the Local Effect of Impurities on the Charge-Density-Wave Phase in TaS₂ by Scanning Tunneling Microscopy

Xian-Liang Wu, Peng Zhou, and Charles M. Lieber

Department of Chemistry, Columbia University, New York, New York 10027

(Received 8 August 1988)

Scanning tunneling microscopy has been used to investigate the effects of titanium impurities on the charge-density-wave (CDW) phase in 1*T*-TaS₂. The average CDW wavelength has been directly measured and found to increase with increasing titanium concentration. However, the local CDW structure distorts significantly in response to the random lattice potential associated with the distorted titanium sites.

PACS numbers: 71.45.Lr, 61.16.Di, 64.70.Kb

The scanning tunneling microscope (STM) is a uniquely powerful tool because it can probe simultaneously with atomic resolution the real-space topographical and electronic properties of conducting interfaces.¹ One interesting problem that the STM is now being used to investigate is the nature of the charge-density-wave (CDW) phases in transition-metal chalcogenide materials.²⁻⁹ To date, the STM has been used to image directly the charge modulation in this state and to determine its periodicity with respect to the underlying atomic lattice.^{5,6,8,9} However, the high spatial resolution of this technique has not been utilized to address the fundamental question of how impurities affect the local properties of the CDW phase. To examine this general problem we have used the STM to investigate the effects of substitutional titanium doping on the CDW state in octahedrally coordinated tantalum disulfide, 1*T*-TaS₂.

There are four distinct CDW phases observed in native 1*T*-TaS₂.^{10,11} The high-temperature incommensurate (IC) phase undergoes a first-order transition at 350 K to a nearly commensurate (NC) state, which transitions to a commensurate (C) phase at 183 K; warming from the C state produces a triclinic nearly commensurate (*T*) phase at 223 K that makes a transition back to the NC phase above 282 K. Previously, DiSalvo and co-workers reported that these phase transitions were strongly perturbed by substitutional doping of the tantalum centers with other metals.^{10,12} For titanium-doped systems Ti_{*x*}Ta_{1-*x*}S₂, the C phase was not observed for $x \geq 0.002$, while the IC to NC transition temperature decreased about 100-K/at.% Ti and was finally lost for $x \geq 0.15$. Suppression of the C and NC phases is believed to be due to randomness in the lattice potential (caused by metal doping); this disorder decreases and ultimately eliminates the energy gain associated with the CDW becoming NC or C with the lattice.^{12,13} In addition, titanium doping, which lowers the average conduction-electron density (d^0 -Ti vs d^1 -Ta), has been found to decrease the magnitude of the diffuse scattering vector observed in electron diffraction experiments.¹⁰ These results provide strong evidence that the size of the Fermi surface determines the CDW wavelength. Despite

these advances, few direct experimental results are available concerning the local effects of metal doping. Hence, it has not been possible to develop a clear microscopic picture of how impurity sites influence the CDW phase in these important systems.

Herein we describe the studies of the local effects of substitutional titanium doping on the CDW state in TaS₂. We have used the STM to determine directly the response of the CDW wavelength to variations in the concentration of titanium, and to determine the local structure of the charge modulation with respect to the atomic lattice in the presence of these impurity sites. Notably, we find that the CDW responds to decreases in the average conduction-electron density, and we also observe large local distortions of the CDW wavelength. These results indicate that the CDW responds on an average to the Fermi-surface geometry, and that the impurity potential can have a large effect on the local CDW structure.

The STM used in this study¹⁴ is a standard single tube design and was operated in the constant current mode. The x, y scan response of the piezo drive was calibrated before all experiments with use of graphite and the CDW wavelength in TaS₂ to better than ± 0.1 Å. The CDW wavelengths reported are averages of the peak-peak separations measured directly from a computer display with standard software. Measurements were also made with the atomic lattice, $a_0 = 3.35$ Å, as an internal standard; both methods yielded similar results. Single-crystal Ti_{*x*}Ta_{1-*x*}S₂ samples were prepared with chemical vapor transport.¹² Elemental analyses verified that the doped crystals were stoichiometric, and Auger electron spectroscopy verified that the surface composition of these samples was similar to the bulk. Images of freshly cleaved crystals were obtained in air under a protective oil at room temperature,⁷⁻⁹ and were recorded from a computer monitor after low-pass filtering the raw data.

A grey-scale image of Ti_{0.1}Ta_{0.9}S₂ recorded at 300 K with a bias voltage of 10 mV (sample positive) and a tunneling current of 2 nA is shown in Fig. 1(a); for comparison an image of 1*T*-TaS₂ recorded under similar conditions is also shown [Fig. 1(b)]. The CDW peaks in

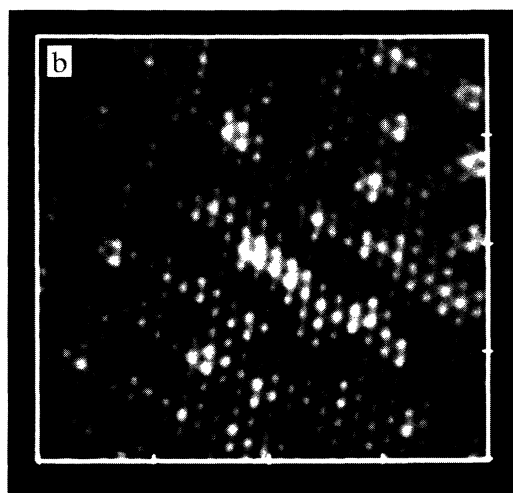
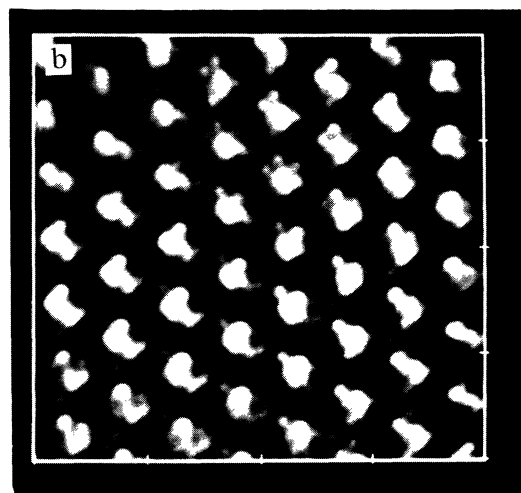
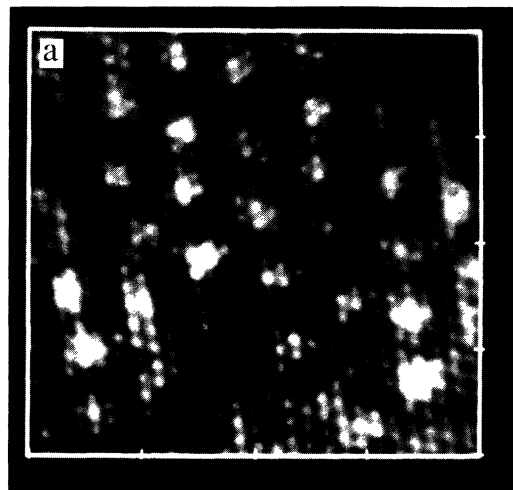
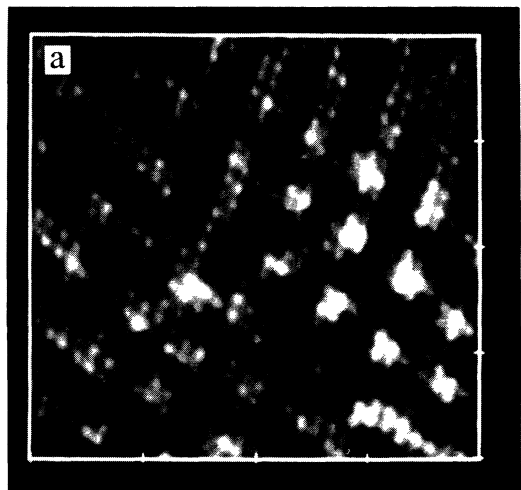


FIG. 1. STM grey-scale images of (a) $\text{Ti}_{0.1}\text{Ta}_{0.9}\text{S}_2$ and (b) 1T-TaS_2 recorded with a 2-nA tunneling current and 10-mV bias voltage (sample positive). White regions are high and dark regions are low. The CDW superlattice is visible as an apparent vertical modulation of the hexagonal atomic lattice, $a_0 = 3.35 \text{ \AA}$. The images are both $80 \times 80 \text{ \AA}^2$.

FIG. 2. $80 \times 80 \text{ \AA}^2$ STM images of (a) $\text{Ti}_{0.08}\text{Ta}_{0.92}\text{S}_2$ and (b) $\text{Ti}_{0.2}\text{Ta}_{0.8}\text{S}_2$ recorded under similar conditions as Fig. 1. The CDW structure in (b) is highly distorted and weak (0.7-\AA vertical modulation).

$\text{Ti}_{0.1}\text{Ta}_{0.9}\text{S}_2$ do not define a regular hexagonal structure in contrast to the periodic structure observed for 1T-TaS_2 .² Although the bulk CDW phase is IC for the Ti-doped sample and NC for 1T-TaS_2 at 300 K,¹² recent STM experiments⁹ have shown that the IC CDW phase in 1T-TaS_2 is very regular, and hence the difference in phases (IC vs NC) cannot explain the contrasting CDW structure observed in these images (Fig. 1). Furthermore, because the underlying atomic lattice maintains a regular hexagonal structure ($a_0 = 3.3 \pm 0.1 \text{ \AA}$) it is unlikely that the observed CDW distortions are due to imaging artifacts. Analysis of the experimental variation in

the CDW wavelength gives a more quantitative measure of the differences between the native and doped samples. The wavelengths $\pm 1\sigma$, determined from the analysis of at least ten images per dopant concentration recorded with use of different samples and tunneling tips, for 1T-TaS_2 and $\text{Ti}_{0.1}\text{Ta}_{0.9}\text{S}_2$ are 11.7 ± 0.1 and $12.9 \pm 1.5 \text{ \AA}$, respectively. The $\pm 0.1\text{-\AA}$ standard deviation determined for the native material is the typical error observed with our instrument; clearly the fifteenfold larger deviation for the $\text{Ti}_{0.1}\text{Ta}_{0.9}\text{S}_2$ samples is intrinsic to the doped material. We suggest that the irregular CDW structure is a result of distortions in direct response to the random lattice potential associated with the titanium dopant sites.

To investigate further the effects of these impurity sites we have imaged the CDW phase in samples containing different titanium concentrations. Images of $\text{Ti}_{0.08}\text{Ta}_{0.92}\text{S}_2$ and $\text{Ti}_{0.2}\text{Ta}_{0.8}\text{S}_2$ are shown in Figs. 2(a) and 2(b), respectively; the bulk CDW phase is IC for these samples at 300 K.¹² The local CDW structure is also distorted for these Ti-doped samples, although, the underlying atomic lattice remains regular. Analysis of the distortions in the CDW structure for at least ten images of both $\text{Ti}_{0.08}\text{Ta}_{0.92}\text{S}_2$ and $\text{Ti}_{0.2}\text{Ta}_{0.8}\text{S}_2$ samples yields wavelengths $\pm 1\sigma$ of 12.4 ± 1.0 and 13.4 ± 1.9 Å, respectively, with both variances at least an order of magnitude larger than determined for 1T-TaS₂. In addition, the variances for the three Ti-doped samples increase with larger values of $x(\text{Ti})$. Since disorder in the lattice potential should also increase over this range of x ,^{10,12} these results support the idea that the local CDW distortions are driven by the random lattice potential. It is unlikely that our observations are due to lattice vacancies because the samples are stoichiometric.

These results clearly show large variations in the local

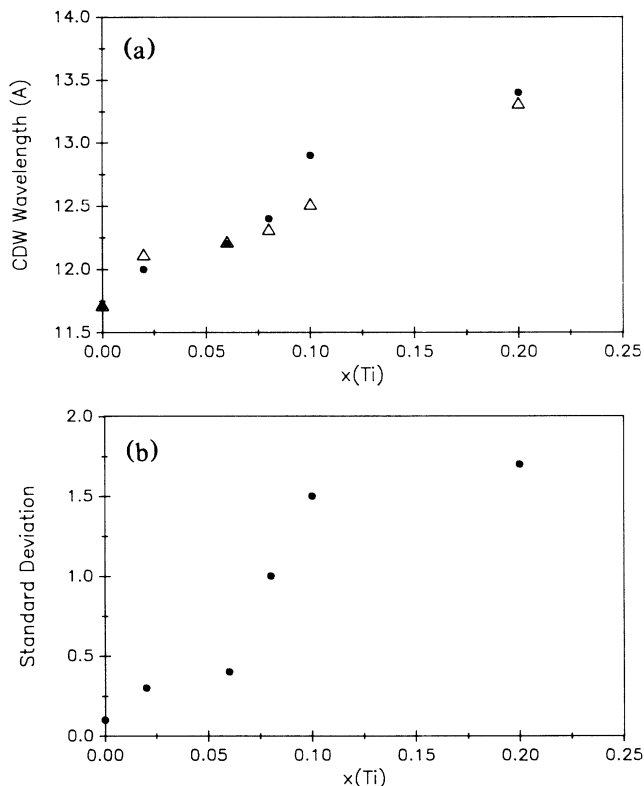


FIG. 3. (a) A plot of the average CDW wavelength vs titanium concentration determined directly with the STM (●) and by diffraction (Δ) (Ref. 10). (b) A plot of the standard deviation in the wavelength for the STM measurements. The typical instrumental error is 0.1 Å; larger values determined for $x(\text{Ti}) \geq 0.08$ are intrinsic to the doped samples.

CDW wavelength for $x(\text{Ti}) = 0.08, 0.1$, or 0.2 ; however, it is also of interest to determine the average wavelength as a function of titanium concentration or, within the rigid-band approximation, the size of the Fermi surface. The average CDW wavelengths measured in this STM investigation and those previously determined from electron diffraction studies¹⁰ increase with increasing titanium concentration [Fig. 3(a)], as expected in response to a decrease in the size of the Fermi surface.¹⁵ We note that these STM results are the first direct (real-space) measure of such changes. In contrast to the diffraction studies we have been unable to image reproducibly the CDW in samples with $x(\text{Ti}) \geq 0.4$ because the amplitude of the CDW decreases with increasing $x(\text{Ti})$.^{8,16} The decreasing amplitude is consistent, however, with local distortions of the CDW when one considers the mechanism of imaging the CDW. Tersoff¹⁷ has shown that the large CDW corrugations observed for 1T-TaS₂ can be attributed to nodes in the surface wave function arising from the three symmetry related CDW's. These singularities will be smoothed and the apparent corrugations reduced when the hexagonal symmetry is broken by the local distortions that we observe.

Comparison of the experimental variance for the CDW wavelength in all of the Ti-doped samples examined in our studied [Fig. 3(b)] gives further insight into the nature of the impurity effect. The variance in the CDW wavelength is close to the instrumental limit (± 0.1 Å) when $x(\text{Ti}) \leq 0.06$, but is significantly larger for samples containing greater dopant concentrations. The difference between these two regimes is immediately evident in the STM images; the CDW in $\text{Ti}_{0.06}\text{Ta}_{0.94}\text{S}_2$

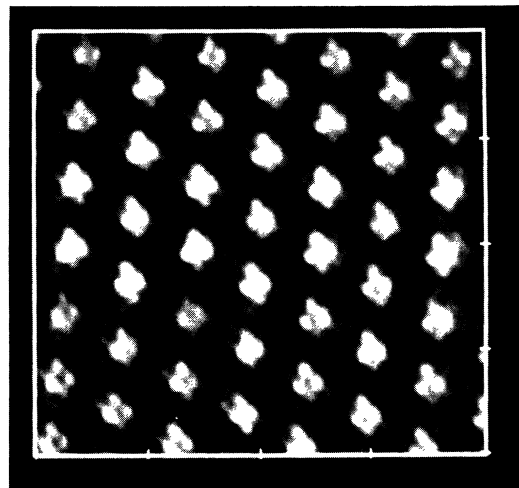


FIG. 4. An 80×80 -Å² image of $\text{Ti}_{0.06}\text{Ta}_{0.94}\text{S}_2$ recorded under conditions similar to Fig. 1. The CDW phase appears to be commensurate in this image, with the same trigonal array of atoms at each CDW maxima.

(Fig. 4) is clearly more regular than the images where $x(\text{Ti}) \geq 0.08$. This behavior is expected because in the lightly doped samples, which are in the bulk NC phase at 300 K,¹⁸ the CDW has partially locked in to the lattice; hence, distortions in response to the random potential are energetically too costly. However, in the IC phase the CDW is not pinned to the lattice and can gain free energy by distorting in response to the disordered Ti sites. Such distortions were proposed theoretically over ten years ago by McMillan,¹⁹ but these STM results represent the first direct experimental evidence supporting this prediction.

Finally, we note that the CDW structure in Fig. 4 appears commensurate, although the bulk sample is NC. This image has the same trigonal array of atoms at each CDW maxima as expected for the C phase,^{5,9,10} and contrasts images we have obtained for NC TaS₂ and images of other $x=0.06$ samples.^{8,20} Although bulk C structures have not been detected for $x(\text{Ti}) > 0.002$,¹⁰ the Fermi surface is in fact better suited to the commensurate $\sqrt{13}a_0$ superlattice when $x(\text{Ti}) \approx 0.03$. Thus, on a local scale, as probed in the STM experiment, the energetic gain for lock-in to the C phase must be sufficient to overcome the random impurity potential. At higher concentrations the Fermi-surface geometry is appropriate for larger commensurate CDW superlattices [i.e., 4×4 at $x(\text{Ti}) = 0.2$], although, such phases have not been detected previously. Our STM results are similar in that large ordered domains have not been imaged; however, $4a_0 \times 4a_0$ CDW superlattices extending for 2-3 unit cells have been observed for $x(\text{Ti}) = 0.1, 0.2$ [e.g., Fig. 1(a), right].

In summary, this study provides the first local measurements of the effects of titanium impurities on the CDW phase in 1T-TaS₂. We have observed large distortions of the local CDW structure in response to the random impurity potential, and we have directly shown that the average CDW wavelength responds to changes in the Fermi-surface geometry. Investigations of the energetics for the local CDW distortions and studies of the local electronic structure in these doped materials are in progress. Such STM studies should provide data necessary for developing microscopic models of the CDW phases in these materials.

The authors acknowledge discussions with F. DiSalvo,

surface analyses by M. Schmidt, and J. V. Waszczak and P. Rauch for providing us with several of the samples. X.-L.W. acknowledges support from Ciba-Geigy, and C.M.L. acknowledges support from the Dreyfus Foundation and the National Science Foundation.

¹R. M. Tromp, R. J. Hamers, and J. E. Demuth, *Science* **234**, 304 (1988).

²R. V. Coleman, B. Drake, P. K. Hansma, and G. Slough, *Phys. Rev. Lett.* **55**, 394 (1985).

³C. G. Slough, W. W. McNairy, R. V. Coleman, B. Drake, and P. K. Hansma, *Phys. Rev. B* **34**, 994 (1986).

⁴R. V. Coleman, W. W. McNairy, C. G. Slough, P. K. Hansma, and B. Drake, *Surf. Sci.* **181**, 112 (1987).

⁵B. Giambattista, A. Johnson, R. V. Coleman, B. Drake, and P. K. Hansma, *Phys. Rev. B* **37**, 2741 (1988).

⁶R. V. Coleman, B. Giambattista, W. W. McNairy, C. G. Slough, P. K. Hansma, and B. Drake, *J. Vac. Sci. Technol. A* **6**, 338 (1988).

⁷X.-L. Wu and C. M. Lieber, *J. Am. Chem. Soc.* **110**, 5200 (1988).

⁸X.-L. Wu, P. Zhou, and C. M. Lieber, *Nature (London)* (to be published).

⁹R. E. Thomson, U. Walter, E. Ganz, J. Clarke, A. Zettl, P. Rauch, and F. J. DiSalvo, *Phys. Rev. B* (to be published).

¹⁰J. A. Wilson, F. J. DiSalvo, and S. Mahajan, *Adv. Phys.* **24**, 117 (1975).

¹¹S. C. Bayliss, A. M. Ghorayeb, and D. R. P. Guy, *J. Phys. C* **17**, L533 (1984).

¹²F. J. DiSalvo, J. A. Wilson, B. G. Bagley, and J. V. Waszczak, *Phys. Rev. B* **12**, 2220 (1975).

¹³D. E. Moncton, F. J. DiSalvo, J. D. Axe, L. J. Sham, and B. R. Patton, *Phys. Rev. B* **14**, 3432 (1976).

¹⁴Nanoscope, Digital Instruments, Inc., Santa Barbara, CA.

¹⁵H. W. Myron and A. J. Freeman, *Phys. Rev. B* **11**, 2735 (1975).

¹⁶The CDW amplitudes for the $x(\text{Ti}) = 0, 0.1, \text{ and } 0.2$ samples are 4, 1, and 0.7 Å, respectively.

¹⁷J. Tersoff, *Phys. Rev. Lett.* **57**, 440 (1986).

¹⁸Variable temperature resistivity measurements have confirmed that the IC-NC transition occurs above 300 K in these samples.

¹⁹W. L. McMillan, *Phys. Rev. B* **12**, 1187 (1975).

²⁰The angle between the CDW superlattice and atomic lattice can be used to distinguish the NC and C phases (12° and 13.9° , respectively); however, within experimental error we cannot use this criteria to distinguish the CDW phase.

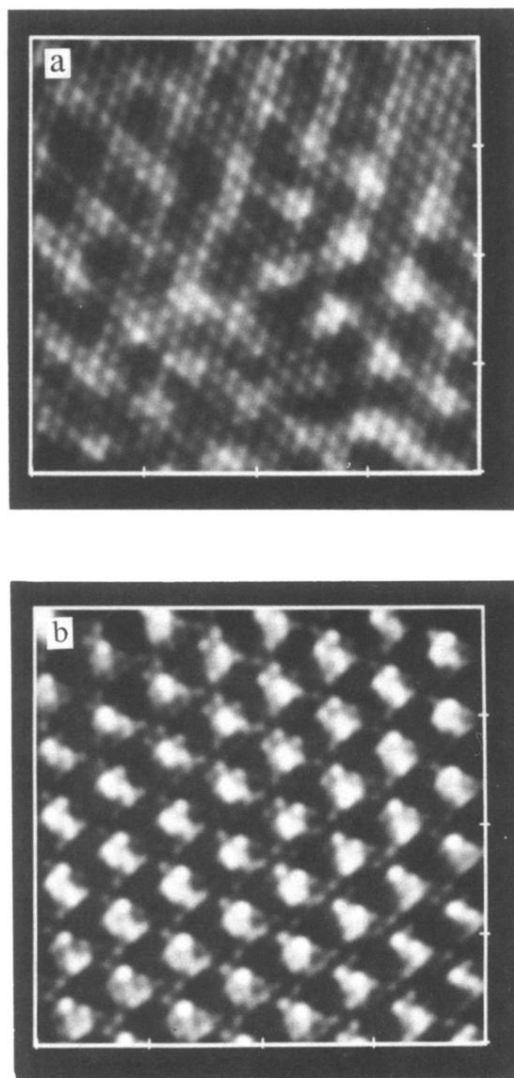


FIG. 1. STM grey-scale images of (a) $\text{Ti}_{0.1}\text{Ta}_{0.9}\text{S}_2$ and (b) $1T\text{-TaS}_2$ recorded with a 2-nA tunneling current and 10-mV bias voltage (sample positive). White regions are high and dark regions are low. The CDW superlattice is visible as an apparent vertical modulation of the hexagonal atomic lattice, $a_0 = 3.35 \text{ \AA}$. The images are both $80 \times 80 \text{ \AA}^2$.

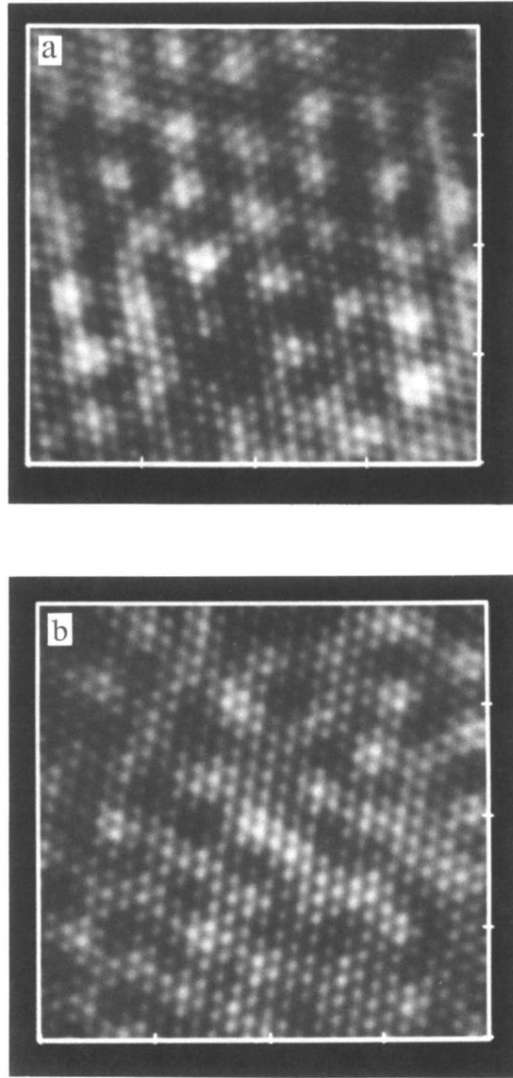


FIG. 2. $80 \times 80\text{-\AA}^2$ STM images of (a) $\text{Ti}_{0.08}\text{Ta}_{0.92}\text{S}_2$ and (b) $\text{Ti}_{0.2}\text{Ta}_{0.8}\text{S}_2$ recorded under similar conditions as Fig. 1. The CDW structure in (b) is highly distorted and weak (0.7-\AA vertical modulation).

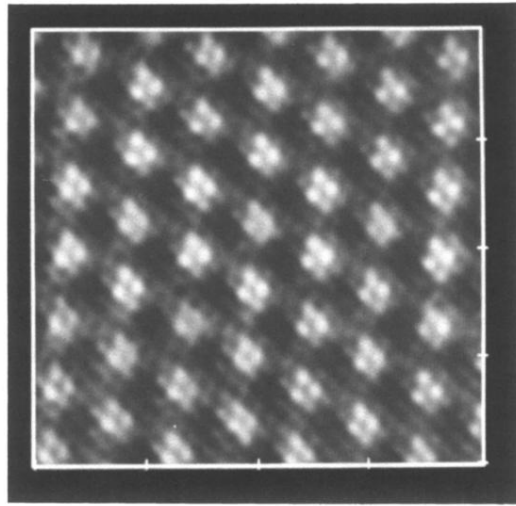


FIG. 4. An $80 \times 80 \text{-}\text{\AA}^2$ image of $\text{Ti}_{0.06}\text{Ta}_{0.94}\text{S}_2$ recorded under conditions similar to Fig. 1. The CDW phase appears to be commensurate in this image, with the same trigonal array of atoms at each CDW maxima.